AteqTERT expression and specific tissue activity in a 2-year-old complete plant in Agave tequilana *in field conditions*

Z. De la Torre Espinosa, Emmanuel Ávila De Dios, Felipe Sánchez Teyer & Enrique Castano

Brazilian Journal of Botany

ISSN 0100-8404

Braz. J. Bot
DOI 10.1007/s40415-020-00642-3

Springer

Brazilian Journal of Botany
https://doi.org/10.1007/s40415-020-00642-3

GENETICS & EVOLUTIONARY BIOLOGY - ORIGINAL ARTICLE

AteqTERT expression and specific tissue activity in a 2-year-old complete plant in *Agave tequilana* in field conditions

Z. De la Torre Espinosa[1,2] · Emmanuel Ávila De Dios[3] · Felipe Sánchez Teyer[2] · Enrique Castano[1]

Received: 3 March 2020 / Revised: 27 July 2020 / Accepted: 29 July 2020

Abstract

Telomerase is a specialized enzyme that attributes to maintaining and lengthening of telomeric length as its primary function. This ribonucleoprotein complex requires two minimum subunits for its *in vivo* function: the TERT amino acid subunit and TER its ribonucleic subunit. Crystallographic studies have shown that stable interaction between subunits and their domains is essential during the active phase. Plants and humans have shown to be tissue specific and dependent on cell proliferation. In *Arabidopsis thaliana* (L.) Heynh, the expression of AtTERT was determined to be necessary for activity. The objective of this work is to perform the *in silico* characterization of TERT in *Agave tequilana* F.A.C. Weber and evaluate the expression of TERT and the specific tissue activity in 2-year-old plants. To this end, we use the transcriptome library of *A. tequilana* (Ávila de Dios unpublished data) in TPM and qTRAP. We observe in this work that the consensus sequence shows all the specific domains of the TERT subunit. Additionally, we carried out the *in silico* prediction of the structural model of AteqTERT. The model presents the characteristic TERT ring of the crystallized models in active state of telomerase, biological annotations were observed, such as heavy metals Mg^{2+}, NUC and CH1, and finally we note that, there is no correlation between TERT expression in TPM and telomerase activity in 2-year meristematic tissue.

Keywords *In silico* characterization · Quantitative activity of telomerase (qTRAP) · Three-dimensional protein modeling · Trascriptomic assembly library (TSA)

1 Introduction

Telomerase is a specialized enzyme necessary for the maintenance of telomeric length, and consequently, it is essential to provide genomic stability in the cell (Wyatt et al. 2010; Kim and Kim 2018). Telomerase can have two different roles of action, such as bind to telomeric sequences for telomeric lengthening and "repair" non-telomeric sequences of the chromosomal tears produced by *novo* telomeres, first observed by Barbara McClintock on corn chromosomes (Greider 2010). Telomerase is a reverse transcriptase and requires two subunits for its function *in vivo*; the amino acidic subunit of telomerase TERT (Telomerase Reverse Transcriptase), responsible for the synthesis of telomeric DNA due to its catalytic capacity (Masutomi et al. 2000; Blackburn and Collins 2011); telomerase RNA (TER/TR), a subunit responsible for the recognition of repeated telomeric motif (Collins 2008). Likewise, crystallographic studies of active telomerase show that the stability in the interactions between TER-TERT telomerase subunits and TERT subunit

Electronic supplementary material The online version of this article (https://doi.org/10.1007/s40415-020-00642-3) contains supplementary material, which is available to authorized users.

✉ Enrique Castano
enriquec@cicy.mx

[1] Unidad de Bioquímica y Biología Molecular de Plantas, Centro de Investigación Científica de Yucatán, A.C, Calle 43 No. 130, Colonia Chuburná de Hidalgo, Mérida, Yucatán, Mexico

[2] Unidad de Biotecnología, Centro de Investigación Científica de Yucatán, A.C, Calle 43 No. 130, Colonia Chuburná de Hidalgo, Mérida, Yucatán, Mexico

[3] Unidad de Ingeniería Genética, Centro de Investigación y Estudios Avanzados del Instituto Politécnico Nacional, Km 9.6 Libramiento Norte Carretera Irapuato – León, Irapuato, Guanajuato, Mexico

Published online: 10 August 2020

domains is essential during their active phase (Jiang et al. 2018).

The TERT subunit has four main domains; the RT domain has the catalytic capacity, TRBD domain responsible for the union between TER and the RT domain, domain, C-terminal domain, and the N-terminal domain (Zvereva et al. 2010). The telomerase RNA subunit regions are necessary for its function *in vivo*. The RNA motif recognizes telomeric DNA and initiates the synthesis of *de novo* telomeric DNA and the 5′ and 3′ limit elements that flank the template RNA (Chen and Greider 2003), and during the telomerase activation phase, these elements positively affect the efficiency of the telomerase, providing nucleotide stability and adding nucleotides to nascent DNA during telomeric DNA synthesis (Greider and Blackburn 1985; Shippen-Lentz and Blackburn 1989; Min and Collins 2010; Lai et al. 2001; Chen and Greider 2003; Zhang et al. 2011). Finally, the critical pseudoknot element in the TER structure, necessary for the correct orientation of the duplex, generates the union between the warm RNA motif and the active site of telomerase (Gilley and Blackburn 1999). Therefore, the viability of the telomerase RNA structure will depend on the conformations of the pseudoknot and the stem-loop (Gilley and Blackburn 1999; Blackburn and Collins 2011).

This functional holoenzyme requires stable associations in the ribonucleic complex; it reported that to observe the active telomerase, it required transcription of the TERT subunit, the formation of the RNA, and the correct assembly of the protein complex (Lai et al. 2001; Witkin and Collins 2004; Eckert and Collins 2012). During the active phase, it shows that stability in the interactions between the TER—TERT telomerase subunits, and the TERT subunit domains are essential, e.g., for RNA/protein association, an RNA binding domain (TRBD) is required, and start its active phase (Witkin and Collins 2004; Collins 2008; Blackburn and Collins 2011). Likewise, this association promotes the repetition of the capacity for addiction, a unique characteristic of telomerase. In turn, this capacity for addition is attributed to for the IFD motif inside to RT motif and the CTE domain, which gives rise to the conformation "thumb" of telomerase. Studies on the functional characteristics in TERT reveal that; the RT, CTE and NTE domains cooperate with binding to RNA, and the other available regions throughout the enzyme may be interacting with other proteins or helping to facilitate dimerization during the synthesis process (Lai et al. 2001; Collins 2006; Min and Collins 2010). Structural studies show that the N-terminal domino (TEN) has DNA binding capacity, and others to non-specific RNAs also show revels that the TRBD domain represents a second RNA interaction site in the CP and T motifs (Gillis et al. 2008; Mitchell et al. 2010).

Currently, the structural elucidation of telomerase in *Tetrahymena thermophila* Nanney & McCoy and *Homo sapiens* Linneo, allowed us to understand how the interaction of each of the regions of TER in TERT happens and their functionality occurs in the active state (Nguyen et al. 2018, Jiang et al. 2018). E.g., in *Tetrahymena thermophila*, the crystallization by Cryo-Em allowed to observe, that the mechanism of all telomerase elements interacts with TERT to active the complex. TER domain *t*/pk can contact with TERT forming a closed circle that is carried out by the stem 1 wrapping the TERT ring, leaving one of the boundary elements of the monocatenary region in the front of the ring, and the pseudoknot in the back on the CTE domain acting as a molecular coupler for keep attached to the complex. In the same way, crystallographic studies in humans, this region (similar to TER domain) is essential for the correct formation of pseudoknot, the addition of nucleotides, the proper processing of telomerase during replication and indispensable for the functioning of the enzyme (Wang et al. 1998; Chang et al. 2002; Jiang et al. 2018).

In plants, no crystallographic reports have been generated so far for the ribonucleic complex. Therefore, we are unaware of the structural organization and interactions in plant telomerase. However, is known that active telomerase in different plant tissues is highly represented in tissues with active division and downwards in differentiated tissues such as leaves, stems, and flowers, show to be species and specific tissue, observed in some species such as *Nicotiana tabacum* L., *Glycine max* (L.) Merr, *Daucus carota* L., *Brassica oleracea* L., *Zea mays* L. and *Hordeum vulgare* L. (Fajkus et al. 1996; Fitzgerald et al. 1996; Killan et al. 1998). Likewise, it observed that telomerase is dependent on the concentration of growth regulators, and it is suggested that auxins influence the phosphorylation or dephosphorylation of the complex to modulate its activity in the cell cycle (Oguchi et al. 2004).

In functional studies of the TERT subunit, the linear sequences of TERT in some species are characterized as: *Scilla peruviana* L, *Doryanthes excelsa Corrêa*, *Ornithogalum virens* Ker. Gawl, *Iris tectorum* Maxim, *Zea mays* L., *Arabidopsis thaliana* (L.) Heynh, *Nicotiana tabacum* L. and *Oryza sativa* Roshev (Oguchi et al. 1999, 2004; Sýkorová et al. 2006a). In *Arabidopsis thaliana* besides from the linear characterization of sequence, employing by Southern blot, it is identified that for this species a unique copy of the AtTERT gene in the divergent genome and is suggested that the expression of AtTERT is essential for telomerase activity because the telomerase activity and expression of AtTERT is abundant in meristematic tissue compared to leaves (Oguchi et al. 1999). However, in plants, there is evidence that differs from that observed in *Arabidopsis thaliana*, as in the monocot species *Oryza sativa*, which shows that telomerase activity is abundant in meristems and low in leaf. At the same time, in the OsTERT gene, five alternative spliced transcript variants were expressed similarly in all

of their tissues (Oguchi et al. 1999, 2004). Therefore, these studies reflect that the regulatory mechanisms of the TERT gene in plants, like other eukaryotic species, are divergent.

In our group, we carried out studies of active telomerase throughout the vegetative development of the leaves under field conditions 1–6 years of age, and we observed that telomerase activity associated with cellular activities such as cell elongation, division, and differentiation. We also observed high telomerase activity throughout the growth phase, while telomere length is maintained during this phase, indicating that telomerase contributes telomeric maintenance (Rescalvo-Morales et al. 2016; De la Torre-Espinosa et al. 2020). There have also been studies of the dynamics in telomeric length in different tissues from 1 to 3 years of age, observing that telomeric length is tissue specific with shorter telomeres in differentiated and elongated tissues in tissues with active division (Rescalvo-Morales et al. 2019). In *A. tequilana*, we do not know whether telomerase activity and TERT expression are tissue specific as observed in telomeric tissue-specific length previously analyzed in tissues of the same age.

Therefore, the objectives of this work are; *in silico* characterization of TERT to evaluate the expression of TERT in the TSA library tissue specific of *A. tequilana* at 2 years of age, measure telomerase activity in tissues of the same age, and preliminarily analyze whether there is a correlation between TERT expression and active telomerase. For characterization of the AteqTERT consensus sequence, we carried out the identification of domains and a structural prediction to know if its biological function was characteristic of other enzymes with similar functions. In the expression of AteqTERT, the tissue-specific transcriptome library was consulted *A. tequilana* made in the laboratory of June—Simpson by Ávila de Dios (unpublished data). Finally, for telomerase activity, quantitative analysis of telomerase activity (qTRAP) was performed in plants with the same age from the transcriptomic library.

2 Materials and methods

Isolation *in silico* and amplification of exon nine of the TERT sequence in *Agave tequilana* (AteqTERT) – For the identification of the candidate sequence of the gene that codes for the TERT subunit in *Agave tequilana*, we carried out a TBLASTn with a sequence of *Oryza sativa* as a query (OsTERT, Uniprot ID Q8LKW0) against a deposited transcriptomic database from *A. tequilana* in NCBI (Gross et al. 2013).

The partial region of the catalytic site that corresponds to exon nine we located into AteqTERT sequence and specific primers are designed (supplementary material) and amplified by PCR following the indications of the enzyme Invitrogen® Taq DNA polymerase (Cat. No. 10342046), using genomic DNA as a template, which we obtained following the Dellaporta method (1998). The PCR products were cloned using TOPO ® TA Cloning ® PCR (Cat No. K4600-01), and we made a positive selection isolating clones that grew in the Luria–Bertani selective medium supplemented with 50 µg ml^{-1} ampicillin and 40 mg ml^{-1} X-gal.

Finally, the obtained sequences were analyzed employing a sequence alignment integrating the AteqTERT consensus sequence applying the neighbor-joining method using MUSCULE and UPGMA.

Analysis of the amino acid and structural sequence of the AteqTERT sequence – To study the AteqTERT amino acid sequence, we used the ORF finder bioinformatic Expasy resource portal (https://web.expasy.org/translate/) to identify the start codon. Subsequently, for the search of conserved regions in the AteqTERT counting sequence, we aligned the sequences with other TERT sequences reported for plants and as external groups mammals and yeast, the phenogram showed we obtained by applying the neighbor-joining method using MUSCLE and UPGMA. Finally, the identification of the conserved domains of the AteqTERT sequence with two bioinformatics tools; ScanProSite (https://prosite.expasy.org/scanprosite) and Geneious®11.0.3 (Restricted) java version 1.8.0 (Kearse et al. 2012), the characteristic of amino acid motifs was identified manually.

For the structural prediction of the AteqTERT sequence, the iterative threading assembly refinement (I-TASSER) was used, an automated platform frequently used for structural prediction, and it performs the combination of several computational structural prediction techniques https://zhanglab.ccmb.med.umich.edu/I-TASSER/. This computational method (I-TASSER) consists in 5 stages, and in each of the stages, a refinement of the modeling is performed, reported in detail by Ambrish (Roy et al. 2010), generates a total of 5 three-dimensional models as a result of structural alignment, and assembly simulation, to later make an inference in biological function, comparing the estimated models with reported criticized proteins. The estimation of the prediction precision is based on the modeling confidence score; for this report, we chose model 1, which was the model that obtained the best confidence interval.

For the visualization of the selected model and the biological annotations using the program "UCSF Chimera—A visualization system for research and exploratory analysis" (Pettersen et al. 2004), the characteristic TERT domains were located, and the biological annotations were analyzed to know the biological function sequence of AteqTERT.

Two-year RNA-seq analysis in different tissue – For the estimation of tissue-specific expression, we consulted the assembled transcriptomic library, obtained by Illumina

sequencing, in different tissues and the stages of development of *A. tequilana*, by Ávila de Dios at the Simpson CINVESTAV-Irapuato Laboratory. Extraction, preparation, and TSA library assembly are described in detail by (De Dios et al. 2019).

RSEM calculate expression, by default, automates the alignment of the readings with the reference transcripts to estimate abundance and its credibility intervals in NCBI with Bowtie 2 (Fig. Sup. 5). These scripts are integrated into the Trinity toolkit to facilitate execution and estimate the abundance of transcripts or expression https://github.com/trinityrnaseq/wiki/Trinity-Transcript-Quantification#rsem-output. The AteqTERT sequence was used as a reference, and the readings were mapped into the transcripts using Bowtie 2. This script allowed us to map short sequences into the transcriptomics libraries, aligning the RNA seq readings with the reference script sequence (RSEM—reference); these aligned reads were used to estimate abundance. Simultaneously, read mapped sequences are aligned with the NCBI database and homologies are identified in other species deposited in the database (Grabherr et al. 2011; De Dios et al. 2015; Zavala-García et al. 2018).

– Expression levels shown are in transcripts per million, as a result of normalization applied to the readings, where gene length is first normalized and then sequencing depth is normalized. This normalization facilitates the comparison in the proportion of the readings assigned to each gene and allows the comparison between different genes or tissues shown in Table 1. For the statistical analysis, we performed ANOVA to observe the differences between the all tissues used. Statistical evaluation and graphics performed with GraphPad Prism version 6.0.

Vegetal material – The plants *A. tequilana* were collected at the "Mayapan" hacienda located in Valladolid, Yucatán. Collected 6-month-old plants were transplanted into pots and placed in a greenhouse for a year and a half. We divided the plant material into middle, basal, central leaf, meristem, and root (Fig. 4a). The tissue of the collected leaves was divided into three different sections: internal apical (IA), internal basal (IB), and external apical (EA), according to the cytological characterization of a young and adult leaf, which shows that the internal basal region has the highest number of cells in G_0, and the internal apical region has more variation in the name of cells in G2, Palomíno et al. (2004). The plant material was stored at − 80 until its use.

TRAP assay – For the telomerase activity assay (TRAP), extraction of active protein, we performed following the indications described above by Fitzgerald et al. (1996) and Sýkorová et al. (2003). Protein concentration was determined in the soluble fraction of the telomerase enriched protein extract (TEX) using the Bradford method (Ismail 1976). For amplification of the products generated by the elongation, we add to the reaction mixture: 200 ng μl^{-1} of the TEX protein extract, 1 µl of 10 µM ml $^{-1}$ of reverse primer (HUTPR: 5´-CCG AAT TCA ACC CTA AAA CCC TAA ACC CTA AAC CCC-3´; Sykorova et al. 2006a, b) and two units of Taq polymerase (Invitrogen ®), during 35 cycles of 95 °C/30 s, 65 °C/30 s, 72 °C/30 s, followed by an extension final at 72 °C/5 min. TRAP products were run on 12.5% PAGE in 0.5x TBE and stained with Syber safe® 1x. The gels scanned with ChemiDoc XRS + Imager (# 170-8265), Bio-Rad. We used conventional TRAP assay to evaluate active telomerase in all samples before quantifying in qTRAP.

QTRAP assay – Quantitative measurement of telomerase activity was performed using the SYBR Green Master (Applied Biosystems), used as template, and forward primer

Table 1 Shows the alignment component in the transcriptomic library in the tissues, the sequence with which it has homology in the NCBI, the size of the sequence of the RNA reads, number of amino acids aligned with the database with the homologous sequence, and the representation of the tissue transcript in TPM

Component	Homologous	Component length (nt)	Alignment length (a.a)	Similarity percentage	TPM leaf	TPM roots	TPM meristems
comp71164_c0_seq1	Oryza sativa Japonica Group]	840	204	49	0	0	3.322399648
comp19507_c0_seq1	NA	765	NA	NA	0	0	2.847771127
comp7782_c0_seq1	Telomerase reverse transcriptase-like [Glycine max]	913	162	72	1.85823419	1.42567518	5.220913733
comp51444_c0_seq1	Telomerase reverse transcriptase-like [Glycine max]	460	147	57	0.464558547	0	2.847771127
comp76970_c0_seq1	Oryza sativa Japonica Group	347	113	53	0	0	1.423885564
				Total in TPM =	2.32279	1.425675	15.6627412

TS21 and TELPR have a reverse primer, and the concentration of each primer in the reaction mixture was 0.25 µM ml $^{-1}$. After the extension stage for 45 minutes at 26 °C and enzymatic inactivation (15 minutes at 95 °C), the extension products by telomerase were amplified in 30 cycles of 30 s at 95 °C, 60 s at 60 °C. (At the end of this step, fluorescence was measured.) For the determination of the standard curve, dilutions containing 500 ng, 200 ng, 100 ng, 50 ng, and 25 ng µl^{-1} of the TEX protein extract were used of apical meristem tissue with active cell division, and each dilution was made in triplicate.

For the positive control of telomerase activity, we used 200 ng µl^{-1} TEX for both meristematic tissue and root tips, for the different tissues analyzed, with the same concentration of 200 ng µl^{-1}. The qTRAP assay was analyzed by real-time PCR Rotor-Gene 3000 (Qiagen) software 2.1.0.9. The values of Ct and the relative telomerase activity were calculated using the delta–delta Ct method. The normalization was carried out following the method described by Pfaffl (2001) and normalized against the Ct values obtained we used the positive control of telomerase activity. For comparison with different tissues, leaf, root, and meristem, we use root tips as normalizer of the Ct value, and the middle, basal, and central leaf, and meristematic tissue were used as positive control. Statistical evaluation and graphics were performed with GraphPad Prism version 6.0.

3 Results and discussion

TERT *in silico* identification of *A. tequilana* – The subunits that are indispensable for the *in vivo* function of telomerase are TERT, and because of this, we explore the gene that encodes TERT in *A. tequilana* using as a query the TERT sequence characterized in *Oryza sativa* (Oguchi et al. 2004), in RNA-seq TSA library of *A. tequilana* deposited at the NCBI data bank (Gross et al. 2013), and we obtained a 3525 *bp* cDNA sequence size. To corroborate the identity, we align the sequence obtained with all sequences deposited into NCBI data back, and we observe similarity with TERT sequences in plants in the order Asparagales, such as *Scilla peruviana* species with 88% identity percentage followed by *Doryanthes excelsa* with 86%, and *Asparagus officinalis* L. with 82% (Sup.Fig. 1a). These percentages of identity indicate the consensus nucleotidic sequence that belongs to the sequence of the gene that encodes the TERT subunit (Sup.Fig. 1).

To ensure that we isolate the correct sequences TERT, we identify the specific exons of sequences TERT (Supplementary material) and the exon nine amplified by PCR to partial region of the catalytic site into RT domain of the telomerase subunit (Fig. 1a, b). The approximate size of sequences was between 750 and 1200 *pb* with combination of primers Fw_Exo9, Fw_Exo 9.a and Rv_Exo 10 and was deposited in the base of NCBI DNA data.

The sequence similarity analysis for exon nine shows an identity percentage of 89% with the consensus sequence AteqTERT—RNA-seq and 82% for the Asparagales species (data not shown). Since we are using DNA as a template, we perform an additional nucleotide alignment with AteqTER. We observe intronic regions in the experimental sequences obtained, that explains differences in percentage of identity and the divergence with the alignment sequences we used. The amplification of the catalytic domain, exons identification, and determination of the presence of the AteqTERT nucleotide sequence in *A. tequilana*, helps to continue with the linear and structural analysis of the AteqTERT amino acid sequence.

Sequence analysis *in silico* of the AteqTERT sequence – The consensus amino acid sequence of AteqTERT have an approximate size of 1175 amino acids, as it is known the size of TERT varies slightly between species, e.g., *Oryza sativa* 1260 *a.a.* (Oguchi et al. 1999, 2004), *Zea mays* 1188 *a.a* (Sýkorová et al. 2006a), *Arabidopsis thaliana* 1123 *a.a* (Oguchi et al. 1999), *Scilla peruviana* 1227 *a.a* (Sýkorová et al. 2006a), *Iris tectorum* 1295 *a.a* (Sýkorová et al. 2006a). Sequence similarity analysis by constructing a phenogram showed that the AteqTERT counting sequence has a 96% identity percentage with Asparagales TERT sequences such as *Scilla peruviana*, *Allium cepa* L., *Iris tectorum*, and *Hosta rectifolia* Nakai which indicates that the amino acid sequence is conserved for the order Asparagales, this is consistent with that reported by Sykorová (Fig. 2a) (Sýkorová et al. 2006a; Fajkus et al. 2016). Likewise, we observed that the identity percentage of 86% in the comparison of monocot species with dicot species, and 74% in the comparison of TERT sequences of plants with TERT sequences of mammals we used as external groups; *Homo sapiens,* and mouse (Fig. 2a). This analysis shows that the sequence TERT is divergent sequences but has conservation in some regions in the TERT amino acid sequence.

We know the TERT sequences has four specific domains and shared among all divergent TERT sequences of eukaryotic species, the degree of conservation of these regions depends on the domain. Previous studies have described that the C-terminal region where the RT domain in charge of catalytic capacity is more conserved among eukaryotic species than the N-terminal domain where is located TRBD, which is the domain responsible for the interaction between the amino acid subunit and telomerase RNA (Bryan et al. 1998; Wick et al. 1999; Oguchi et al. 2004; Sýkorová et al. 2006b).

In this study, we observed the characteristic motifs of the TERT subunit as; NTE, TRBD, and RT, during the identification of the domains in the TERT sequence, the

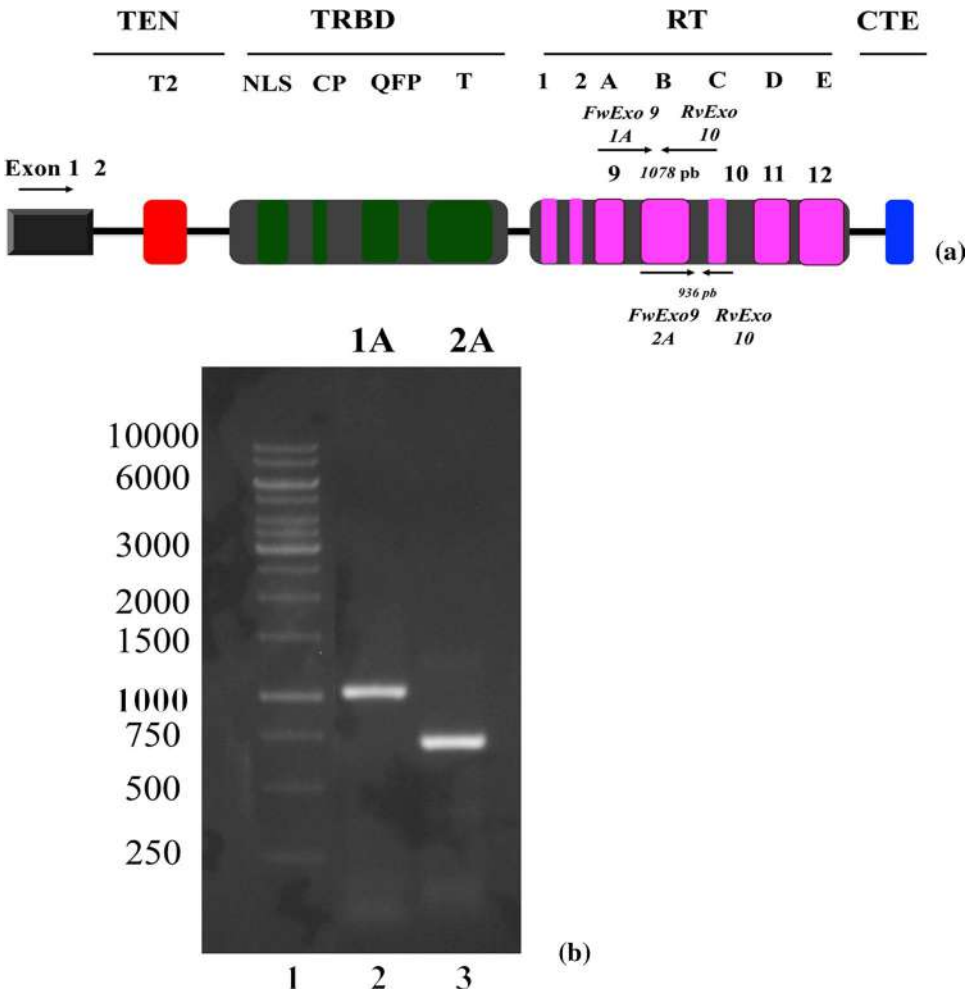

Fig. 1 Nucleotide identification, oligonucleotide design and PCR amplification of exon 9 of the *AteqTERT* consensus sequence. **a** Schematic representation of the TERT gene and nucleotide identification of exon 9 correspond to the partial region of the catalytic site, we design two direct oligonucleotides for exon 9; FwExo9 (1A)—FwExo9 (2A), and a single RvExo9 reverse oligonucleotide; **b** amplified PCR products using 20 ng of genomic DNA as tempering; **1**. molecular weight marker, **2**. PCR product with the combination FwExo9 (1A) + Rv Exo9, **3**. PCR product with the combination FwExo9 (2A) + RvExo9

characteristic motifs found are GQ, QFP, GLLL, and T motifs (Oguchi et al. 1999, 2004; Sýkorová et al. 2006b). These motifs are located in the T2, TRBD, and C-terminal domains, respectively. The T motif is an amino acid sequence that is specific for telomerase (Fig. 2b), the presence of this motif it possible to differentiate telomerase from the rest of the viral retro-transcriptases (RTs), and this motif is part of the TRBD domain (Figs. 2b, 3d) (Bryan et al. 1998; Oguchi et al. 2004; Sýkorová et al. 2006b). Interestingly, we observed that the consensus sequence of AteqTERT have the amino acid change of leucine (L) or phenylalanine (P) to tryptophan (W) in motif C, in position two upstream of the double catalytic DD of the TERT subunit, this amino acid change previously reported for some Asparagale*s* species (Sýkorová et al. 2006a). The N-terminal region of the TERT subunit presents more variation in comparison with the rest of the domains, this region is highly conserved in the species Asparagales, and this includes the sequence consensus of *A. tequilana* (Sýkorová et al. 2006b; Petrova et al. 2018). Finally, we observed a total of 12 exons in AteqTERT that are similar to observed *Nicotiana tobacco* (Sýkorová et al. 2012), *Oryza sativa* (Oguchi et al. 2004), and *Arabidopsis thaliana* (Oguchi et al. 1999). Nevertheless, the lack of experimental evidence limits us to conclude if it is the total number of exons in *A. tequilana*, since the genomic structure of TERT can vary in the number of exons, e.g., the TERT subunit in *Homo sapiens* has a total of 16 exons (Harrington et al. 1997; Wick et al. 1999), so we need to perform an experimental characterization in cDNA of *A. tequilana*, to conclude if it is composed of a total of 12 exons or more. However, with the identification of the specific domains of the TERT subunit, we managed to confirm that the consensus sequence obtained corresponds to the chain that codes for the TERT subunit in *A. tequilana*.

Structure analysis of AteqTERT – After we made of domain identification, we perform the structural prediction to infer the architecture of its structure and biological function of the consensus sequence. This value was calculated based on the alignment of the templates, and the convergence parameters of the assembly simulations are represented confidence intervals as C score, TM score and RMSD

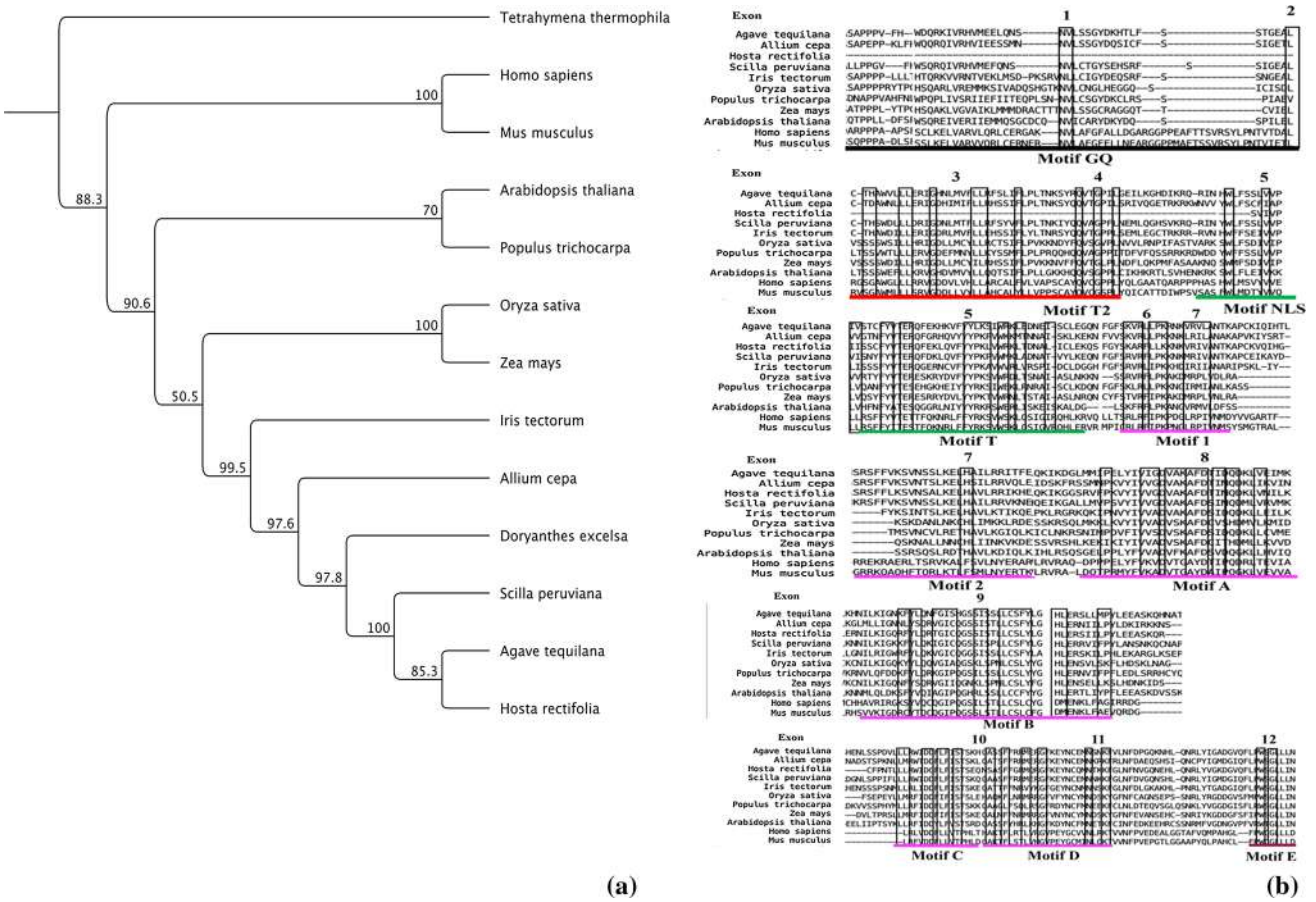

Fig. 2 *AteqTERT* sequence similarity analysis. **a** Phenogram of TERT amino acid sequences reported in different species of plants, mammals and ciliates using UPGMA with a 1000 repetition bootstrap performed in Genius Java Version 1.8.0_112-b15 (64 bit), **b** identification of domains, motifs and exons in the *AteqTERT* sequence using UPGMA with a 1000 repetition bootstrap performed in Genius Java Version 1.8.0_112-b15 (64 bit)

values. We obtained that the model 1 PDB is within the range acceptable with value score $C = -1.15$; the range of acceptable 3D architectural confidence is $[-5, 2]$. The TM-score value $= 0.57 \pm 0.15$ that is the score for comparations between two proteins, and the range confidence acetable is (0, 1) and RMSD $= 12.1 \pm 4.4$ Å, which measures the similarity of the mean square deviation of the three-dimensional sequence of the atomic coordinates of Cα in the PDB models obtained. This value depends on the resolution of the crystallized model with which the structural comparison was made, and the model that presents most significant structural similarity for the AteqTERT consensus sequence was the model 6d6VA, which corresponds to the crystallized telomerase structure in state active in *Tetrahymena thermophila*, which was characterized using cry electron microscopy with a resolution of 4.8 Å. We indicated the location of each of the specific domains of the subunit, colour red for the NTE domain, green for the TRBD domain, magenta for the RT and blue domain for the CTE (Fig. 3a). This analysis showed that the architecture of its structure of telomerase is similar to other polymerases reported and other viral RT's, in a 90° turn in front, it is observed that the TRBD-RT -CTE domains form the unique TERT ring (Fig. 3b). Recently, the catalytic nucleus of telomerase was found in the structure of TERT from *Tetrahymena thermophila* as unique architecture. The RBD, RT and CTE domain form a ring called "TERT ring" linked by a TER loop 4 (L4) that is responsible for the molecular grouping of these domains (Jiang et al. 2018), likewise, in the crystallized structure in *Tribolium Castaneum* Herbst and *Homo sapiens* observed that these three domains have the same particular architecture (Gillis et al. 2008; Mitchell et al. 2010; Nguyen et al. 2018). Still, in this structure, it is not shown if this ring has a specific additional interaction, such as in the case of *Tetrahymena thermophila*.

We found that the active site corresponds to the double Asp in the RT domain at amino acid positions 913 and 914 shown in Fig. 3c. The active site of TERT is between the two laminar beta structures of motif C, and motif D is an alpha-helix structure whose location in the linear sequence

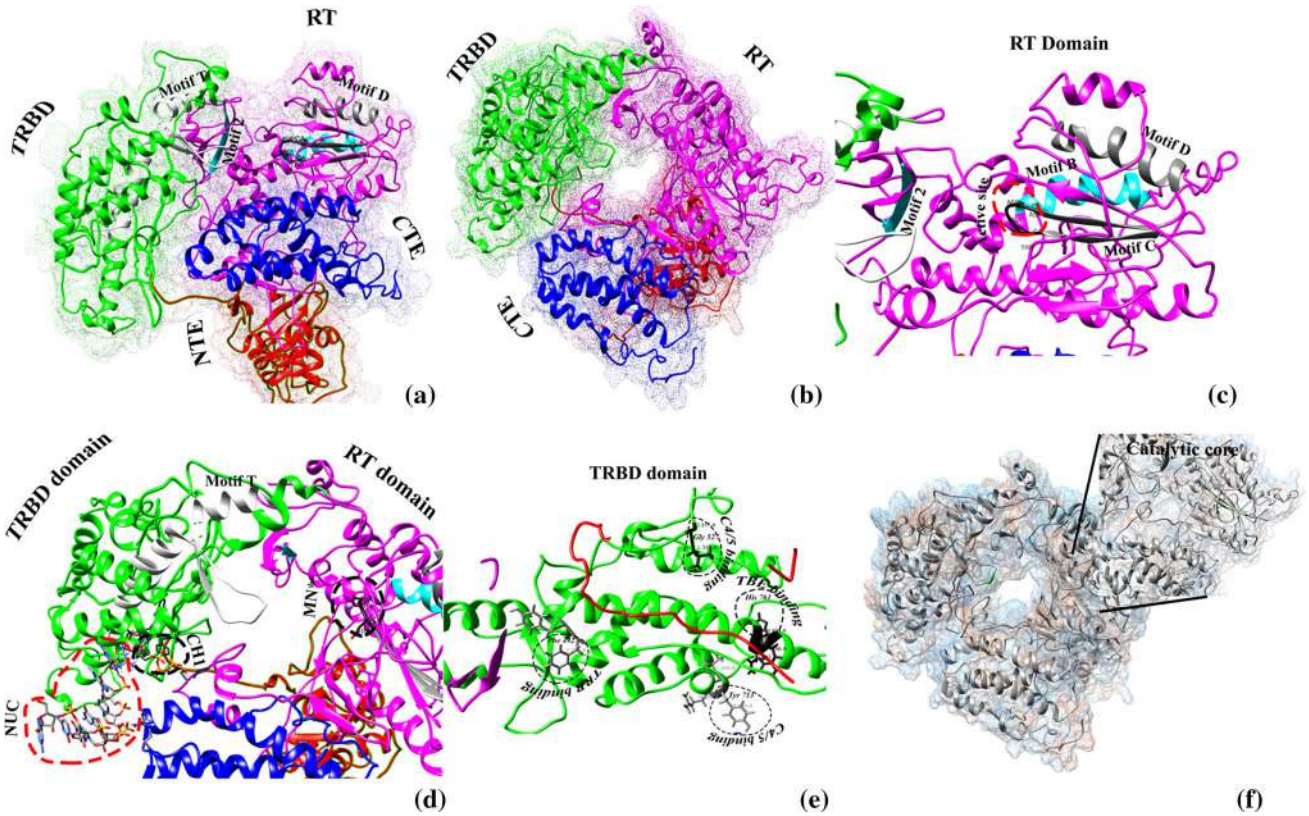

Fig. 3 Modeling of the AteqTERT amino acid sequence. The different colors represent each domain of AteqTERT; the NTE domain—red, TRBD—green, RT—pink and CTE—blue, **a** representation of the 3D surface structure and alpha–beta laminar structure of AteqTERT with the different domains of TERT, **b** interaction of the domains of TERT in surface structure and alpha–beta structure that form the characteristic TERT ring, **c** the conserved motifs adjacent to the active site B, C, D and 2, **d** biological annotations of the ligand binding site in the TRBD domain; to the CH1 ligand (3- deoxycytidine 5- triphosphate) and nucleic acid binding (NUC) and RT domain binding site to MN (Mg^{2+}), **e** TR subunit binding sites in TRBD domain, **f** analysis of the hydrophobicity of the structure where the blue coloration represents the hydrophilic regions and the red coloration the hydrophobic areas, the PDB models of the TERT sequence and the prediction of biological annotations were obtained using the I-TASSER bioinformatics tool, with a C score = −1.15, TM score = 0.57 ± 0.15 and RMSD = 12.1 ± 4.4 Å, the structures we visualized and edited using UCSF Chimera Quick version 1.14

is closest to the catalytic site. However, motif 2, which is the β-laminar structure, and motif B, which is the alpha-helix structure, is structurally closer to the active site (Fig. 3c). In *Tribolium Castaneum* the crystallization of TERT allowed to know that the union between TERT and TER is mediated by motifs 2 and B, due to its location near the active telomerase site (Gillis et al. 2008; Mitchell et al. 2010). Here, we observe that these motifs are close to the catalytic site, but yet to be defined if a TERT motifs for plants has this function. TBE motifs in TRBD are necessary for the interaction of TR with the TERT subunit. They are conserved in the family of these enzymes. Therefore, we identify the TBE and C4/5 binding regions in the TRBD domain in the amino acid sequence (Fig. Sup. 4) and in the structure (Fig. 3e), showing that AteqTERT presents the four amino acids that make up the TBE and C4/5 interaction sites (Fig. 3d), two of the amino acids show conservation for all species, and two species-specific (Fig. Sup. 4).

The analyses carried out by COFACTOR and COACH allowed to infer the biological annotations (biological function) ligand binding sites (Fig. 3d). The analysis of the biological function by COFACTOR showed biological annotations similar to RNA polymerases such as NUC (nucleic acids), CH1 (3′-deoxycytidine-5′-triphosphate), and magnesium (2+), the CH1 and NUC ligands positioned in amino acid residues 429, 430, 440, 443, 444, 445 in the TRBD domain, and the MN ligand observed in the position; 913, 914 which corresponds to the double Asp at the catalytic site of the RT domain (Fig. 3d). The PDB's models with ligand similarity are: 1GX6 for the MN ligand that belongs to the hepatitis C virus RNA polymerase in complex with UTP and manganese (Bressanelli et al. 2011), 3aOhD for the NUC ligand that belongs to the RNA polymerase-Gfh1 complex (Tagami et al. 2010), and finally the PDB 1N38 model for the CH1 ligand that belongs to the complex reovirus polymerase lambda 3 (Tao et al. 2002). These ligands contribute

to the process of RNA synthesis, nucleotide translocation and initiate their enzymatic activity, indicating that possibly the MN ligand observed in the catalytic site is necessary to start the activity of telomerase. The telomerase enzyme is known it is used Mg^{2+} as a cofactor; likewise, the CH1 and NUC ligands observed in the TRBD domain leads us to think that possibly the CH1 ligand may be contributing to the flexibility of translocation of telomeric DNA, and NUC to the synthesis of telomeric DNA. These results of inference in the architecture of its structure and the biological function of the consensus sequence show that it has a similarity with telomerase and other reverse transcriptase enzymes. Recently, elucidated structures of *Tetrahymena thermophila* telomerase the active state contributed in large part to understand how amino acid interactions between each of the TERT domains and the TER telomerase RNA occur (Jiang et al. 2018). Within all these interactions, the TER loop 4 maintains a cluster between the domains of the TERT ring. Subsequently, the t/pk domain of the tempered RNA in telomerase forms a circle on and behind the TERT ring. Limiting the end of the template on the front and the pseudoknot on the back on the CTE domain. TERT—TEN interaction together with RBD and the bottom of the t/pka circle form a flexible structured connector that facilitates the interaction of TEN—TRAP (located in TER), creating a third ring (TEN-RBD-TR-TRAP) (Jiang et al. 2018). This structure physically blocks the TERT ring and sequesters the limiting ends of TER binding. Therefore, the anchor of TBE in RBD is necessary to define the limit of the template and prevent physically that non-repeated template nucleotides move to the active site (Jansson et al. 2015), a few months before Nguyen et al. (2018) observed similar interactions between the domains of the TERT and TR subunits, but, in the case of hTR they observe that it has an elongated P6 region and has two stems that are not observed in *Tetrahymena thermophila*, P6a and P6b, and apparently these regions do not interact with TERT (Nguyen et al. 2018). Finally, the model for telomeric DNA synthesis is in the form of an accordion, limited to understanding and extension to adjacent template ends. In *Trubullium castaneum*, the superposition of TERT-TER, shows bases accessible in the solvent above and adjacent to the active site during the binding of acid nucleic, facilitating the selectivity of the protein (Gillis et al. 2008; Mitchell et al. 2010). The interaction between the substrate DNA in the first region located at the 3′ end and the active site facilitates nucleotide addition. In general, the forces involved in the binding may be hydrophilic interactions. Still, the specificity of binding appears to be controlled by hydrogen bonds, and electrostatic interactions, in the hydrophobicity analysis, show that hydrophobic regions are found mostly in the CTE domain of the AteqTERT structure, near the catalytic site of the enzyme (Fig. 3f), which leads us to think that in this region, it is necessary for the fidelity of the protein.

Finally, the studies in telomerases of different organisms show that telomerases differ in the interaction of each of their domains and their catalytic properties, in processivity, fidelity, and even in some organisms, they function as dimers that could be related to the non-canonical activities of the subunit (Beilstein et al. 2012). Because of this, we consider that in plants there is a great need to conduct studies from a biochemical point of view, in order to understand how this interaction happens.

Telomerase activity and expression of TERT in a 2-year-old *A. tequilana* complete plant – To determine the telomerase activity of *A. tequilana,* the amplification efficiency, a standard curve was made with different concentrations of meristem precipitate extract (TEX) 500, 200, 100, 50, 25 ng μl^{-1}, with an $R^2 = 0.97$ indicating that the Ct value is directly proportional to the level of extract used in the reaction (De la Torre-Espinosa et al. 2020).

Subsequently, we carried out the quantitative analysis of TRAP for complete 2-year *A. tequilana* plants, analyzing the difference in telomerase activity between central, middle, and basal leaf was analyzed, using *A. tequilana* root tips as a positive control (Fig. 4b). We observed differences in active telomerase between the central leaf and the basal leaf with a value of $P = 0.01$ (Fig. 4b). However, in the comparison between the central and the middle leaf, no statistically significant differences were found. The active telomerase pattern is highly represented in the central leaf, followed by the middle leaf; finally, the basal leaf presents the tissue with less activity. After performing the analysis in different leaf positions, the various sections of the middle we analyzed; internal apical (IA), internal basal (IB), and external basal (EB), using meristem as a positive control (Sup. Figure 3b), showing that there are no significant differences between sections IA, IB and EB (Sup Fig. 3b). Moreover, the evaluation of active telomerase in meristem, leaf, and root, using root tips as a positive control, observing high telomerase activity for meristem and leaf, in the root normalization a difference of over three orders of magnitude in comparison with root tips. Therefore, telomerase activity in the root is significantly less than root tips, and we also found significant differences between the meristem and the root with a value of $P < 0.0001$, with a difference in the activity of three orders of magnitude.

In *Agave*, the leaves make up the most substantial proportion of the plant. The development of its leaves is in the form of a rosette. The different positions of the leaves: basal, middle, and central, represent different levels of development in the plant, as demonstrated in other species *Zea mays* (Thomas 2013) For *A. tequilana*; the basal leaf has the highest proportion of its differentiated tissue and is considered

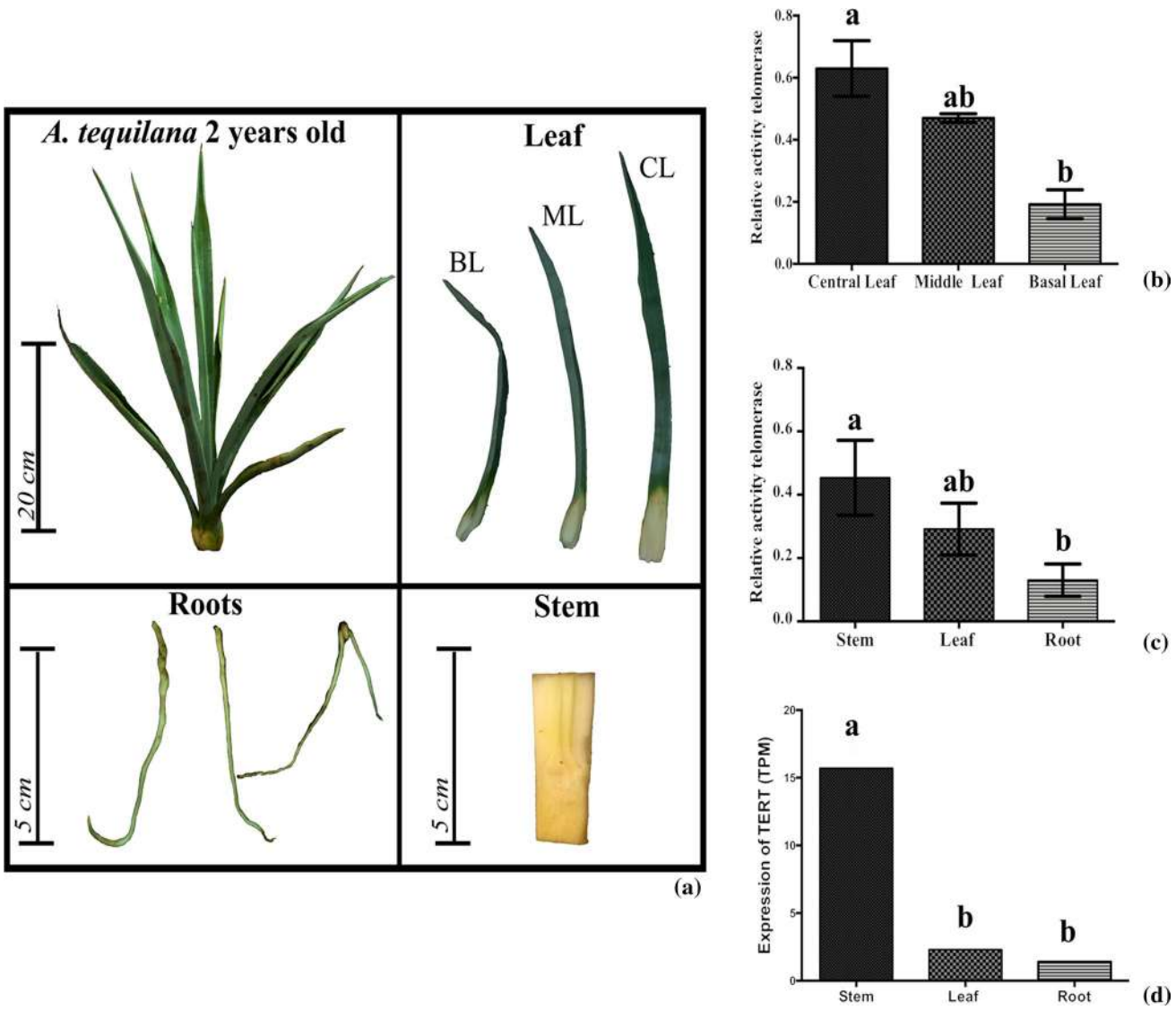

Fig. 4 Specific tissue telomerase activity and expression in 2-year-old complete plants of *A. tequilana.* a different tissues of the whole 2-year-old *A. tequilana* plant, middle leaf (ML), basal (BL), central (CL), roots and meristem; **b** telomerase activity in central, middle and basal leaf; **c** telomerase activity in different tissues, meristem, middle leaf and root, **d** AteqTERT expression in TPM of meristem, leaf and root in 2-year-old *A. tequilana* plants

the oldest leaf, due to its location at the base of the stem; the middle leaf represents the middle part of the stem, and the tissue is in continuous differentiation, and the central leaf is considered the youngest leaf due to its location in the apical region of the stem, adjacent to the meristematic tissue, and is the tissue with the highest proportion of active division, therefore, in this position the leaves are still in formation and growth.

In this report, considering the type of development of its leaves and the analysis of active telomerase between; central, middle and basal leaf, agree that reported in other species such as *Arabidopsis thaliana*, *Oryza sativa*, where active telomerase reported in tissue with a high rate of cell division and with less detection in a differentiated tissue. These results indicate that the telomerase activity in *A. tequilana* leaves is specific for each position. More significant activity is also observed in the meristem, followed by the middle leaf and with low root activity. These results are similar to those previously reported, where telomerase activity is tissue specific and depends on cell proliferation such as *Nicotiana tabacum*, *Glycine max*, *Daucus carota*, *Brassica oleracea*, *Zea mays* and *Hordeum vulgare* (Fajkus et al. 1996; Fitzgerald et al. 1996; Killan et al. 1998). Therefore, telomerase activity in complete plants of *A. tequilana* is tissue specific, active in tissues with high division rates, and less activity in differentiated tissues. Likewise, in previous

reports of telomeric length in *A. tequilana* in tissues with 2 years old, observed that the average length is 24–29 *kb*, the most elongated telomeres are for meristem, followed by central leaf, middle leaf, and the shortest telomeres are detected in; basal leaf and root, concluding that the telomeric length for complete plants is tissue specific. We observe that the activity detected in 2 years agrees with the reported length. We can suggest that for *A. tequilana* at 2 years of age, telomerase is the mechanism by which telomeres lengthened or maintained. This correlation in *Agave* leads us to suggest a specific tissue balance between telomere length and telomerase activity, similar to that observed in maize and barley where telomerase activity is progressively suppressed during the tissue differentiation process, causing telomeres to shorten during this process due to telomere replication.

Finally, we evaluated the gene expression that codes for the TERT subunit in different tissues, to preliminarily analyze whether telomerase activity is related to TERT expression in tissues of the same age (Fig. 4c, d). In this part, we performed the RNA-seq tissue-specific analysis to *A. tequilana* with approximately 2 years. The results of the expression of AteqTERT obtained show that there is high expression in meristematic tissue, followed by leaves and the lowest expression observed in the root. In comparing the expression of TERT in the different tissues analyzed, the expression of the TERT subunit in meristem is six orders of magnitude more significant compared to leaves and eleven times larger than root (Fig. 4c). This study reveals that the pattern observed in the expression of TERT and the pattern of activity is similar, mostly represented in tissues with active division and differentiated tissues with less representativeness. However, when evaluating the comparison of telomerase activity and TERT expression for each tissue, we observe that the telomerase activity between meristems and root show significant differences, also observed, difference in expression of AteqTERT. However, the activity between the meristem and the leaf does not show significant differences in the telomerase activity, and the comparison of expression between meristem and leaf is different by sixfold higher. In this comparison, in leaf tissue under the conditions in which we performed the experiments, there is no correlation between expression and telomerase activity (Fig. 4c, d).

In plants, there are reports such as *Oryza sativa* that focused on determining the correlation between telomerase activity and TERT gene expression, determined that telomerase activity is strictly regulated and dependent on proliferation during development. However, they observed that during the stages of development, there is no correlation between; telomerase activity and TERT expression; these same authors identified that, like *Arabidopsis thaliana*, it presents a single copy of TERT in the divergent genome. However, the mechanisms of genetic regulation of TERT seem to be different between both species. For *Arabidopsis thaliana*, it is determined that the TERT gene is essential for telomerase activity (Oguchi et al. 1999). In *Oryza sativa* OsTERT, the mechanisms involved are its positive regulation or negative that appear to be carried out by the great diversity of alternative splice variants found, a total of eight gene variants that have exon deletion 5,6,7,8 and 11 were identified, during the expression analyzes of the variants of the gene. It is observed that the OsTERT gene variant by exon 11 deletion is more abundant in leaves, a tissue that presents negative telomerase, and the full-length OsTERT variant is abundant in tissues such as callus, cell cultures, or immature embryos with active telomerase (Heller-Uszynska et al. 2002; Oguchi et al. 2004; Chung et al. 2005). Additionally, they observed high levels of TERT expression in tissues with high cell division, suggesting that the gene could probably be participating in cellular activities, independently of telomeric maintenance (Oguchi et al. 2004).

On the other hand, in the divergent genome of *Nicotiana tobacco*, it has been identified that TERT can present more copies of the gene, this species has three copies of the gene, and the expression of each copy of the gene during development modifies the activity of telomerase (Sýkorová et al. 2012; Jurečková et al. 2017). *Agave tequilana* preliminarily observed by analysis of available TSA libraries, fluorescence in situ hybridization, and cDNA present two copies of the gene (data not shown). Therefore, the lack of correlation between the expression of TERT and leaf telomerase activity reveals that the regulatory mechanisms of the TERT gene in *A. tequilana* are involved. Therefore, functional studies in TERT need to be carried out to understand the genetic regulation in this species. Perform an expression analysis of tissue-specific TERT under the same conditions at different stages of development, to identify whether gene copies or alternative splice variants regulate telomerase activity as reported in other species.

Ultimately, in this work, we made the characterization of TERT in *A. tequilana*, to assess whether TERT expression correlates with specific tissue activity in 2-year-old plants. We reported that the consensus sequence presents all the specific domains of the TERT subunit. Additionally, we found that in the *in silico* prediction of the structural model of TERT of *A. tequilana*, it presents the characteristic TERT ring of the crystallized models active state of telomerase in *Tetrahymena thermophila*, *Homo sapiens*, *Trubullium Castenum*, some entertaining biological function were observed, such as heavy metals Mg^{2+}, NUC and CH1 present in other RNA's polymerases or reverse transcripts, and finally we see that, there is no correlation between TERT expression in TPM and telomerase activity in 2-year meristematic and leaf tissues.

Acknowledgements To E. a person essential for my personal and academic development and giving me experimental guidance and knowage on this topic, thanks for sharing your experience and time with me, this project was funded by CONACyT Project CB-2012-180757-Z and by the grant awarded and Goty Bautelpacher, owner of the hacienda "MAYAPAN" farm for the plant material and June - Simpson for access to the RNA - Seq library, for its support and academic time granted.

References

Beilstein MA, Brinegar AE, Shippen DE (2012) Evolution of the *Arabidopsis* telomerase RNA. Front Genet 3:1–8. https://doi.org/10.3389/fgene.2012.00188

Blackburn EH, Collins K (2011) Telomerase: an RNP enzyme synthesizes DNA. Cold Spring Harb Perspect Biol 3:1–9. https://doi.org/10.1101/cshperspect.a003558

Bressanelli S, Tomei L, Rey FA, De Francesco R (2011) Quantifying differences in circulation patterns with probabilistic methods. 8:2011–2011. https://doi.org/10.1128/jvi.76.7.3482

Bryan TM, Sperger JM, Chapman KB, Cech TR (1998) Telomerase reverse transcriptase genes identified in *Tetrahymena thermophila* and *Oxytricha trifallax*. Proc Natl Acad Sci 95:8479–8484. https://doi.org/10.1073/pnas.95.15.8479

Chang JTC, Chen YL, Yang HT et al (2002) Differential regulation of telomerase activity by six telomerase subunits. Eur J Biochem 269:3442–3450. https://doi.org/10.1046/j.1432-1033.2002.03025.x

Chen JL, Greider CW (2003) Template boundary definition in mammalian telomerase. Genes Dev 17:2747–2752. https://doi.org/10.1101/gad.1140303

Chung H, Hishinuma R, Ando S, Sakai S (2005) A possible mRNA splicing mechanism for regulation of telomerase activity in rice (*Oryza sativa* L.). J Plant Biol 48:209–219. https://doi.org/10.1007/BF03030410

Collins K (2006) The biogenesis and regulation of telomerase holoenzymes. Nat Rev Mol Cell Biol 7:484–494. https://doi.org/10.1038/nrm1961

Collins K (2008) Physiological assembly and activity of human telomerase complexes. Mech Ageing Dev 129:91–98. https://doi.org/10.1016/j.mad.2007.10.008

De Dios EA, Vargas ADG, Santos MLD, Simpson J (2015) New insights into plant glycoside hydrolase family 32 in *Agave* species. Front Plant Sci 6:1–14. https://doi.org/10.3389/fpls.2015.00594

De Dios EA, Delaye L, Simpson J (2019) Transcriptome analysis of bolting in *A. tequilana* reveals roles for florigen, MADS, fructans and gibberellins. BMC Genom 20:1–18. https://doi.org/10.1186/s12864-019-5808-9

De la Torre-Espinosa ZY, Barredo-Pool F, Castaño de la Serna E, Sánchez-Teyer LF (2020) Active telomerase during leaf growth and increase of age in plants from *Agave tequilana* var. Azul. Physiol Mol Biol Plants 26:639–647. https://doi.org/10.1007/s12298-020-00781-7

Eckert B, Collins K (2012) Roles of telomerase reverse transcriptase N-terminal domain in assembly and activity of *Tetrahymena* telomerase holoenzyme. J Biol Chem 287:12805–12814. https://doi.org/10.1074/jbc.m112.339853

Fajkus J, Kovařík A, Královics R (1996) Telomerase activity in plant cells. FEBS Lett. https://doi.org/10.1016/0014-5793(96)00757-0

Fajkus P, Peška V, Sitová Z et al (2016) *Allium* telomeres unmasked: the unusual telomeric sequence (CTCGGTTATGGG)n is synthesized by telomerase. Plant J 85:337–347. https://doi.org/10.1111/tpj.13115

Fitzgerald MS, McKnight TD, Shippen DE (1996) Characterization and developmental patterns of telomerase expression in plants. Proc Natl Acad Sci USA 93:14422–14427. https://doi.org/10.1073/pnas.93.25.14422

Gilley D, Blackburn EH (1999) The telomerase RNA pseudoknot is critical for the stable assembly of a catalytically active ribonucleoprotein. Proc Natl Acad Sci USA 96:6621–6625. https://doi.org/10.1073/pnas.96.12.6621

Gillis AJ, Schuller AP, Skordalakes E (2008) Structure of the *Tribolium castaneum* telomerase catalytic subunit TERT. Nature 455:633–637. https://doi.org/10.1038/nature07283

Grabherr MG, Haas BJ, Yassour M et al (2011) Full-length transcriptome assembly from RNA-Seq data without a reference genome. Nat Biotechnol 29:644–652. https://doi.org/10.1038/nbt.1883

Greider CW (2010) Telomerase discovery: the excitement of putting together pieces of the puzzle (Nobel lecture). Angew Chem Int Ed 49:7422–7439. https://doi.org/10.1002/anie.201002408

Greider CW, Blackburn EH (1985) Identification of a specific telomere terminal transferase activity in *Tetrahymena* extracts. Cell 43:405–413. https://doi.org/10.1016/0092-8674(85)90170-9

Gross SM, Martin JA, Simpson J et al (2013) De novo transcriptome assembly of drought tolerant CAM plants, *Agave deserti* and *Agave tequilana*. BMC Genom 14:563. https://doi.org/10.1186/1471-2164-14-563

Harrington L, Zhou W, McPhail T et al (1997) Human telomerase contains evolutionarily conserved catalytic and structural subunits. Genes Dev 11:3109–3115. https://doi.org/10.1101/gad.11.23.3109

Heller-Uszynska K, Schnippenkoetter W, Kilian A (2002) Cloning and characterization of rice (*Oryza sativa* L.) telomerase reverse transcriptase, which reveals complex splicing patterns. Plant J 31:75–86

Ismail AM (1976) A rapid and sensitive method for the quantitation of microgram quantities of protein utilizing the principle of protein-dye binding. Anal Biochem 72:248–254. https://doi.org/10.1016/0003-2697(76)90527-3

Jansson LI, Akiyama BM, Ooms A et al (2015) Structural basis of template-boundary definition in *Tetrahymena* telomerase. Nat Struct Mol Biol 22:883–888. https://doi.org/10.1038/nsmb.3101

Jiang J, Wang Y, Sušac L et al (2018) Structure of telomerase with telomeric DNA. Cell 173:1179–1190.e13. https://doi.org/10.1016/j.cell.2018.04.038

Jurečková JF, Sýkorová E, Hafidh S et al (2017) Tissue-specific expression of telomerase reverse transcriptase gene variants in *Nicotiana tabacum*. Planta 245:549–561. https://doi.org/10.1007/s00425-016-2624-1

Kearse M, Moir R, Wilson A et al (2012) Geneious basic: an integrated and extendable desktop software platform for the organization and analysis of sequence data. Bioinformatics 28:1647–1649. https://doi.org/10.1093/bioinformatics/bts199

Killan A, Heller K, Kleinhofs A (1998) Development patterns of telomerase activity in barley and maize. Plant Mol Biol 37:621–628. https://doi.org/10.1023/a:1005994629814

Kim MK, Kim WT (2018) Telomere structure, function, and maintenance in plants. J Plant Biol 61:131–136. https://doi.org/10.1007/s12374-018-0082-y

Lai CK, Mitchell JR, Collins KL (2001) RNA binding domain of telomerase reverse transcriptase. Mol Cell Biol 21:990–1000. https://doi.org/10.1128/mcb.21.4.990

Masutomi K, Kaneko S, Hayashi N et al (2000) Telomerase activity reconstituted in vitro with purified human telomerase reverse transcriptase and human telomerase RNA component. J Biol Chem 275:22568–22573. https://doi.org/10.1074/jbc.m000622200

Min B, Collins K (2010) Multiple mechanisms for elongation processivity within the reconstituted *Tetrahymena* telomerase holoenzyme. J Biol Chem 285:16434–16443. https://doi.org/10.1074/jbc.m110.119172

Mitchell M, Gillis A, Futahashi M et al (2010) Structural basis for telomerase catalytic subunit TERT binding to RNA template and telomeric DNA. Nat Struct Mol Biol 17:513–518. https://doi.org/10.1038/nsmb.1777

Nguyen THD, Tam J, Wu RA et al (2018) Cryo-EM structure of substrate-bound human telomerase holoenzyme. Nature 557:190–195. https://doi.org/10.1038/s41586-018-0062-x

Oguchi K, Liu H, Tamura K, Takahashi H (1999) Molecular cloning and characterization of AtTERT, a telomerase reverse transcriptase homolog in *Arabidopsis thaliana*. FEBS Lett 457:465–469

Oguchi K, Tamura K, Takahashi H (2004) Characterization of *Oryza sativa* telomerase reverse transcriptase and possible role of its phosphorylation in the control of telomerase activity. Gene 342:57–66. https://doi.org/10.1016/j.gene.2004.07.011

Petrova OA, Mantsyzov AB, Rodina EV et al (2018) Structure and function of the N-terminal domain of the yeast telomerase reverse transcriptase. Nucleic Acids Res 46:1525–1540. https://doi.org/10.1093/nar/gkx1275

Pettersen EF, Goddard TD, Huang CC et al (2004) UCSF Chimera—a visualization system for exploratory research and analysis. J Comput Chem 25:1605–1612. https://doi.org/10.1002/jcc.20084

Pfaffl MW (2001) A new mathematical model for relative quantification in real-time RT-PCR. Nucleic Acids Res 29:e45. https://doi.org/10.1093/nar/29.9.e45

Rescalvo-Morales A, Monja-Mio KM, Herrera-Herrera G et al (2016) Analysis of telomere length during the organogenesis induction of *Agave fourcroydes* Lem and *Agave tequilana* Weber. Plant Cell Tissue Org Cult 127:135–143. https://doi.org/10.1007/s11240-016-1037-y

Rescalvo-Morales A, Monja-Mio KM, Robert ML, Sánchez-Teyer LF (2019) Telomere length in *Agave tequilana* Weber plants during the in vitro to ex vitro transition. Plant Cell, Tissue Organ Cult. https://doi.org/10.1007/s11240-018-1499-1

Roy A, Kucukural A, Zhang Y (2010) I-TASSER: a unified platform for automated protein structure and function prediction. Nat Protoc 5:725–738. https://doi.org/10.1038/nprot.2010.5

Shippen-Lentz D, Blackburn EH (1989) Telomere terminal transferase activity from *Euplotes crassus* adds large numbers of TTTTGGGG repeats onto telomeric primers. Mol Cell Biol 9:2761–2764

Sýkorová E, Lim KY, Kunická Z et al (2003) Telomere variability in the monocotyledonous plant order Asparagales. Proc Biol Sci 270:1893–1904. https://doi.org/10.1098/rspb.2003.2446

Sýkorová E, Leitch AR, Fajkus J (2006a) Asparagales telomerases which synthesize the human type of telomeres. Plant Mol Biol 60:633–646. https://doi.org/10.1007/s11103-005-5091-9

Sýkorová E, Leitch AR, Fajkus J (2006b) Asparagales telomerases which synthesize the human type of telomeres. Plant Mol Biol. https://doi.org/10.1007/s11103-005-5091-9

Sýkorová E, Jurečková J, Mokroš P et al (2012) Three TERT genes in *Nicotiana tabacum*. Chromosom Res 20:381–394. https://doi.org/10.1007/s10577-012-9282-3

Tagami S, Sekine SI, Kumarevel T et al (2010) Crystal structure of bacterial RNA polymerase bound with a transcription inhibitor protein. Nature 468:978–982. https://doi.org/10.1038/nature09573

Tao Y, Farsetta DL, Nibert ML, Harrison SC (2002) RNA synthesis in a cage—structural studies of reovirus polymerase λ3. Cell 111:733–745. https://doi.org/10.1016/s0092-8674(02)01110-8

Thomas H (2013) Senescence, ageing and death of the whole plant. New Phytol 197:696–711. https://doi.org/10.1111/nph.12047

Wang H, Gilley D, Blackburn EH (1998) A novel specificity for the primer-template pairing requirement in *Tetrahymena* telomerase. EMBO J 17:1152–1160. https://doi.org/10.1093/emboj/17.4.1152

Wick M, Zubov D, Hagen G (1999) Genomic organization and promoter characterization of the gene encoding the human telomerase reverse transcriptase (hTERT). Gene 232:97–106. https://doi.org/10.1016/s0378-1119(99)00108-0

Witkin KL, Collins K (2004) Holoenzyme proteins required for the physiological assembly and activity of telomerase. Genes Dev 18:1107–1118. https://doi.org/10.1101/gad.1201704

Wyatt HDM, West SC, Beattie TL (2010) InTERTpreting telomerase structure and function. Nucleic Acids Res 38:5609–5622. https://doi.org/10.1093/nar/gkq370

Zavala-García LE, Sánchez-Segura L, Avila de Dios E et al (2018) Starch accumulation is associated with active growth in *A. tequilana*. Plant Physiol Biochem 130:623–632. https://doi.org/10.1016/j.plaphy.2018.08.011

Zhang Q, Kim N-K, Feigon J (2011) Architecture of human telomerase RNA. Proc Natl Acad Sci USA 108:20325–32. https://doi.org/10.1073/pnas.1100279108

Zvereva MI, Shcherbakova D, Dontsova O (2010) Telomerase: structure, functions, and activity regulation. Biochemistry 75:1563–1583. https://doi.org/10.1134/s0006297910130055